



Available online at www.sciencedirect.com

ScienceDirect

Journal of the Franklin Institute 360 (2023) 6880–6905

www.elsevier.com/locate/jfranklin



Conditional scenario-based model predictive control

Edwin González*, Javier Sanchis, José Vicente Salcedo,
Miguel Andrés Martínez

Instituto Universitario de Automática e Informática Industrial, Universitat Politècnica de València, Valencia, 46022, Spain

Received 29 November 2022; received in revised form 31 March 2023; accepted 13 May 2023

Available online 18 May 2023

Abstract

This paper proposes a novel MPC approach called conditional scenario-based model predictive control (CSB-MPC), developed for discrete-time linear systems affected by parametric uncertainties and/or additive disturbances, which are correlated and with bounded support. At each control period, a primary set of equiprobable scenarios is generated and subsequently approximated to a new reduced set of conditional scenarios in which each has its respective probabilities of occurrence. This new set is considered for solving an optimal control problem in whose cost function the predicted states and inputs are penalised according to the probabilities associated with the uncertainties on which they depend in order to give more importance to predictions that involve realisations with a higher probability of occurrence. The performances of this new approach and those of a standard scenario-based MPC are compared through two numerical examples, and the results show greater probabilities of not transgressing the state constraints by the former, even when considering a smaller number of scenarios than the scenario-based MPC.

© 2023 The Author(s). Published by Elsevier Inc. on behalf of The Franklin Institute.

This is an open access article under the CC BY-NC-ND license

(<http://creativecommons.org/licenses/by-nc-nd/4.0/>)

* Corresponding author.

E-mail address: edgonqu1@alumni.upv.es (E. González).

<https://doi.org/10.1016/j.jfranklin.2023.05.012>

0016-0032/© 2023 The Author(s). Published by Elsevier Inc. on behalf of The Franklin Institute. This is an open access article under the CC BY-NC-ND license (<http://creativecommons.org/licenses/by-nc-nd/4.0/>)

1. Introduction

Model predictive control (MPC), also known as receding horizon control, is widely used in industry [1] and in other sectors [2–6]. This is due to the simplicity of its implementation and its robustness in the control of various processes that can be complex and have many inputs-outputs with constraints to consider. Robust [7,8] and stochastic [8–11] MPC approaches are appropriate strategies for uncertain systems. The robust approach assumes that the uncertainties are unknown, but have known limits, when solving a min-max optimal control problem (OCP) based on the worst-case and where the constraints are required to be satisfied for all cases.

Stochastic model predictive control (SMPC) considers that the uncertainties (bounded or not) are either parametric [12,13], due to external disturbances [14–17] or both [18–20] are stochastic in nature; but the information about how the uncertainties or random variables are distributed is considered as known. These probability distributions in most cases are considered as Gaussian distribution types and whose sequences in time are assumed as independent and identically distributed (i.i.d.). This statistical information is used to solve an OCP based on expected value, where the state and input constraints must be satisfied at least with a defined level of probability. In this way, the worst-case conservatism [21], which does not always occur, is reduced when compliance with constraints is relaxed in probabilistic terms, and in which its transgression is allowed within a permitted level of probability.

Most SMPC approaches in the literature are classified into two groups: deterministic strategies [22–24], and scenario-based or randomised strategies [18,25,26]. Comparisons between techniques of both groups can be found in González et al. [27], Grosso et al. [28], Seron et al. [29]. The deterministic strategies propose an OCP whose cost function is based on the expected value and state constraints defined as probabilistic or chance constraints. The non-convexity of these constraints can make the problem computationally unmanageable. Such probabilistic constraints are converted into deterministic and convex equivalents and make use of the knowledge of the first two statistical moments of the random variables by tightening [22] the hard constraints offline. This results in an OCP similar to that of a classic MPC in structure and computational tractability.

On the other hand, in the scenario-based strategies, this expected cost function is approximated by the sample average by generating at each control period an appropriate set of random realisations, also called scenarios [30,31], of the uncertainties for all the instants of the prediction horizon. These realisations are included in a standard convex OCP with constraints that must be fulfilled for all the generated scenarios. The quality of the solution or its approximation to the original problem is conditioned by the number of realisations used to solve the OCP.

These scenario-based schemes have been used in practical applications for the control of processes related to autonomous vehicles [32], thermal comfort in buildings [3], management of water resources [28,33] or microgrids [6,34]. This is due to its flexibility in allowing the online addition of new statistical information since this is not required for offline constraint tightening as in the case of deterministic approaches. In addition, if empirical data on uncertainties are available, scenarios can be selected from such data; hence, it is not required to know how the random variables are distributed.

Such advantages imply a higher cost related to the time spent by the OCP to compute a solution, which increases or decreases in line with the number of scenarios. Moreover, as discussed in Schildbach et al. [19] and Farina et al. [11], when a small number of random

scenarios are considered, there is a possibility that some are far from the reality of the process and, consequently, the optimal controls calculated can cause erroneous behaviour in the closed-loop system. In [18], this number is calculated as the minimum number of scenarios required to satisfy the constraints in the states, according to an allowed level of probability of transgression.

To improve the cost function, while maintaining a permitted level of constraint transgression for a sufficiently high number of generated scenarios, some scenarios of this total can be discarded [35] from the OCP constraints. In [19], a sample-removal pair is proposed and this consists of calculating a pair, given as a minimum number of scenarios to consider in the cost function and a maximum number of scenarios to discard from the constraints in the states, in accordance with risk acceptability level of constraint violation. These scenario removal schemes can cause an increase in the solution time because in addition to demanding a high value of scenarios; they require an appropriate algorithm [35] to identify unlikely scenarios to be removed from the constraints, which could result in an OCP that is computationally expensive to solve. In the scenario tree-based MPC [36–39] approach, which is based on multi-stage stochastic optimisation, a tree-shaped structure is built according to different realisations of the disturbances, where each node or bifurcation of the tree represents a certain future instant which is associated with the probability of being reached and its control action, given the uncertainty. Every possible future path in this tree, beginning in the current state, is considered a scenario. Therefore, a reduced number of scenarios made up of those that are most likely to occur can be considered if an improvement is needed in the solution time [37,40].

Challenges such as improving the probabilities of constraint satisfaction and computational tractability of a scenario-based MPC discussed above motivated the development of the new scenario-based MPC approach introduced in this work. In summary, the contributions are stated as follows:

1. A novel scenario-based SMPC approach called conditional scenario-based model predictive control (CSB-MPC), developed for discrete-time linear systems. Most SMPC approaches consider systems with either strictly additive or parametric uncertainties; and whose realisations are independent or correlated in time. This work addresses systems with bounded parametric and/or additive uncertainties featuring a correlation between some or the whole set of random variables.
2. An algorithm that adapts the conditional scenario CS reduction method to the SMPC framework to approximate a primary set of equiprobable scenarios into a reduced set of CSs (that preserve the main characteristics of this primary set) with their probabilities of occurrence. The CS concept was proposed as an approximation to the two-stage stochastic mixed-integer linear programming problems, where a scenario consists of a realisation of the random vector composed of the existing set of uncertainties, which are correlated. In contrast, in the MPC context, a scenario consists of a sequence of various realisations of that vector.
3. A cost function where the probabilities of occurrence of the realisations of the uncertainties are used as weights that penalise the states and inputs associated with these realisations. This mitigates the effect of unlikely scenarios on the optimal control problem by giving more relevance to states and inputs with higher probabilities of occurrence.
4. The CSB-MPC has a higher probability of constraints satisfaction than a standard scenario-based MPC for the same number of scenarios and offers a similar solution time, sometimes

shorter, when a smaller sized primary set is used. With the above in mind, using a CSB-MPC with a smaller number of scenarios is a viable option when a quicker solution time is required but with no performance loss.

The remaining structure of this paper is organised as follows. Section 2 addresses the type of system to be considered and the formulation of the scenario-based MPC. The concept of conditional scenario, its adaptation to MPC context and the proposed CSB-MPC approach are presented in Section 3. Through simulations of two numerical examples, the proposed approach and scenario-based MPC performances are discussed in Section 4. Finally, conclusions are drawn in Section 5.

2. Problem statement

In this section, the model of the system to be considered and the formulation of a Scenario-based MPC are described.

2.1. System dynamics

Consider an uncertain linear time-invariant (LTI) system whose discrete state-space dynamic is given by Eq. (1a) in which its input $u \in \mathbb{R}^{n_u}$ is ruled by the state feedback control law Eq. (1b), and subject to constraints in states Eq. (1c) and inputs Eq. (1d), for a given instant of time $i \in \mathbb{N}_0$

$$x_{i+1} = A(\delta_i)x_i + B(\delta_i)u_i + Gw(\delta_i) \tag{1a}$$

$$u_i = Kx_i + v_i \tag{1b}$$

$$x \in \mathbb{X} \tag{1c}$$

$$u \in \mathbb{U} \tag{1d}$$

where vectors $x \in \mathbb{R}^{n_x}$, $w(\delta) \in \mathbb{R}^{n_w}$ and $v_k \in \mathbb{R}^{n_u}$ represent the state, exogenous disturbances and the decision variables, respectively. $A(\delta) \in \mathbb{R}^{n_x \times n_x}$ is the state matrix, $B(\delta) \in \mathbb{R}^{n_x \times n_u}$ is the system input matrix, $G \in \mathbb{R}^{n_x \times n_w}$ is a matrix that reflects the effect of $w(\delta)$ on the system states, and $K \in \mathbb{R}^{n_u \times n_x}$ is a feedback matrix that stabilises the system. Constraints Eqs. (1c)–(1d) are expressed as linear inequalities (e.g., $F_x x \leq b_x$ for Eq. (1c), and $F_u u \leq b_u$ for Eq. (1d)).

Vector $\delta \in \mathbb{R}^{n_\delta}$ is random, bounded and is composed of each of the parametric or additive uncertainties, represented by the random variable $\xi_n \forall n \in \{1, 2, \dots, n_\delta\}$, present in the system such that $\delta = [\xi_1, \xi_2, \dots, \xi_{n_\delta}]^\top$. Thus, $A(\delta)$, $B(\delta)$ and $w(\delta)$ are random and bounded since all or some of their elements are functions of δ .

Assumption 1. Correlated Uncertainties: For a given instant of time $i \forall i \in \{0, 1, \dots, \}$ some or the whole set of uncertainties $\{\xi_{1,i}, \xi_{2,i}, \dots, \xi_{n_\delta,i}\}$ of the random vector δ_i are correlated in that instant. The vector δ has a multivariate normal distribution and bounded support \mathbb{W}_δ . Any sequence $\{\delta_0, \delta_1, \dots\}$ is independent and identically distributed (i.i.d.) and can be obtained from experimental data or by means of a random number generator.

2.2. Scenario-based MPC

At each sampling time and with the availability of the current state measure, SMPC strategies [9,11,41] use a process model such as Eq. (1a), whose uncertainties are stochastic in nature and with known probability distributions, to solve an optimal control problem. This OCP solution generates the sequence of future controls to lead states toward the origin or a desired operating point.

According to the above, let k be the current time, \hat{x}_k the state measured at that moment and N the prediction horizon. Model Eq. (1a) and its input Eq. (1b), based on dual paradigm [42], are used to predict the future states $x_{i+1|k} \forall i \in \{0, 1, \dots, N - 1\}$ and inputs $u_{i|k}$, for N steps ahead of k ; where the subscript $i|k$ indicates the predicted value of the variable for the instant i , based on the information available at time k , and $x_{0|k} = \hat{x}_k$

$$x_{i+1|k} = A(\delta_{i|k})x_{i|k} + B(\delta_{i|k})u_{i|k} + Gw(\delta_{i|k}) \tag{2a}$$

$$u_{i|k} = Kx_{i|k} + v_{i|k}. \tag{2b}$$

In SMPC schemes, predictions Eqs. (2a) and (2b) are commonly incorporated into the cost function $J(\hat{x}_k, v_k) = \mathbb{E} \left[\sum_{i=0}^{N-1} (\|x_{i|k}\|_Q^2 + \|u_{i|k}\|_R^2) + \|x_{N|k}\|_P^2 \right]$ based on the expected value [22–24], denoted by \mathbb{E} , in which $\|y\|_W^2 = y^T W y$. In the scenario-based approaches [18,19,26], this expected cost function is approximated by the sample average Eq. (3), which consists of an average of the predicted trajectories of the states over a horizon N , for a finite number of M realisations of the uncertainties $\{\Delta_k^{[1]}, \Delta_k^{[2]}, \dots, \Delta_k^{[M]}\}$ called scenarios [30,43]

$$\hat{J}(\hat{x}_k, v_k) = \frac{1}{M} \sum_{j=1}^M \left[\sum_{i=0}^{N-1} (\|x_{i|k}^{[j]}\|_Q^2 + \|u_{i|k}^{[j]}\|_R^2) + \|x_{N|k}^{[j]}\|_P^2 \right] \tag{3}$$

where matrices $\{Q \in \mathbb{R}^{n_x \times n_x} | Q \geq 0\}$, $\{R \in \mathbb{R}^{n_u \times n_u} | R > 0\}$ and $\{P \in \mathbb{R}^{n_x \times n_x} | P > 0\}$ penalise the states, inputs, and the terminal state $x_{N|k}$, respectively. Scenarios $\Delta_k^{[j]} \forall j \in \{1, 2, \dots, M\}$ represent the predictions of the uncertainties for N steps $\Delta_k^{[j]} = \{\delta_{0|k}^{[j]}, \delta_{1|k}^{[j]}, \dots, \delta_{N-1|k}^{[j]}\}$ such that $\delta_{i|k}^{[j]} = [\xi_{1,i|k}^{[j]}, \xi_{2,i|k}^{[j]}, \dots, \xi_{n_s,i|k}^{[j]}]^T$. Thus, the j th predicted trajectory is obtained by evaluating Eqs. (2a) and (2b) with $\Delta_k^{[j]}$, fulfilling $x_{0|k}^{[j]} = \hat{x}_k$ and the same decision variables $\{v_{k|k}, v_{k+1|k}, \dots, v_{k+N-1|k}\}$ for all M . This is

$$x_{i+1|k}^{[j]} = A(\delta_{i|k}^{[j]})x_{i|k}^{[j]} + B(\delta_{i|k}^{[j]})u_{i|k}^{[j]} + Gw(\delta_{i|k}^{[j]}) \tag{4a}$$

$$u_{i|k}^{[j]} = Kx_{i|k}^{[j]} + v_{i|k}. \tag{4b}$$

For every time k , the control problem in the scenario-based MPC framework is to minimise Eq. (3) fulfilling the constraints on states Eq. (1c) and inputs Eq. (1d) for all $x_{i+1|k}^{[j]}$ and $u_{i|k}^{[j]}$, respectively, and in the terminal state $x_{N|k}^{[j]} \in \mathbb{X}_T$ [44,45] if required. The aforementioned is addressed in OCP Eq. (5), whose solution yields the optimal controls $v_k^* = \{v_{0|k}^*, v_{1|k}^*, \dots, v_{N-1|k}^*\}$

$$\min_{v_{0|k}, v_{1|k}, \dots, v_{N-1|k}} \hat{J}(\hat{x}_k, \mathbf{v}_k) \tag{5a}$$

s.t.

$$x_{i+1|k}^{[j]} = A(\delta_{i|k}^{[j]})x_{i|k}^{[j]} + B(\delta_{i|k}^{[j]})u_{i|k}^{[j]} + Gw(\delta_{i|k}^{[j]}) \tag{5b}$$

$$u_{i|k}^{[j]} = Kx_{i|k}^{[j]} + v_{i|k} \tag{5c}$$

$$x_{i+1|k}^{[j]} \in \mathbb{X} \tag{5d}$$

$$u_{i|k}^{[j]} \in \mathbb{U} \tag{5e}$$

$$x_{N|k}^{[j]} \in \mathbb{X}_T \tag{5f}$$

$$x_{0|k}^{[j]} = \hat{x}_k \tag{5g}$$

$$\forall i \in \{0, 1, \dots, N - 1\}, \quad \forall j \in \{1, 2, \dots, M\}. \tag{5h}$$

Using the receding horizon (RH) strategy [46], only the first element of \mathbf{v}_k^* is applied to the process in that time (i.e., $u_k = u_{0|k} = K\hat{x}_k + v_{0|k}^*$), repeating the OCP at the next sampling time. OCP Eq. (5) can be stated as a quadratic programming (QP) problem with a global optimum due to the quadratic and convex nature of Eq. (3), the linear model Eq. (1a), and linear constraints Eqs. (5d)–(5f)

Assumption 2. Optimal Control Problem: Matrices Q and R are defined by the designer. For the uncertain system Eq. (1a) K and P can be obtained by solving an eigenvalues problem (EVP) from a quadratic stability analysis using Lyapunov’s approach [7,47,48], that makes the $A(\delta_i) + B(\delta_i)K$ matrix strictly stable. The sets \mathbb{X} , \mathbb{U} and $\mathbb{X}_T \subset \mathbb{X}$ are convex sets that contain the origin in their interiors. For any instant of time the current state \hat{x}_k is assumed to be measurable, the set $\Delta_k^{[j]} \forall j \in \{1, 2, \dots, M\}$ is generated according to Assumption 1, and the OCP is assumed to find a feasible solution at that instant.

2.2.1. Number of scenarios

Establishing an appropriate number of M possible realisations of uncertainties to be considered to solve the OCP Eq. (5) is essential. This is because optimal solutions can be obtained for a large number of realisations but at the expense of an excessive computational burden. On the other hand, if number of realisations is small, an accurate approximation of the uncertainty cannot be achieved. For this reason, a certain balance [43] between the numerical tractability and quality of its solution is required. In [18,43], this number is calculated according to a defined probability level $p \in [0, 1]$ of non-violation of constraints in the states $\mathbb{P}[x_{i+1|k} \in \mathbb{X}] \geq p$,

a very low confidence level $\beta \in [0, 1]$ (e.g., $\beta = 10^{-9}$) and the number of decision variables $d = n_u N$

$$\sum_{j=0}^{d-1} \binom{M}{j} (1-p)^j p^{M-j} \leq \beta \tag{6}$$

where M is the minimum value that satisfies Eq. (6) or by its approximation $M \geq (2/(1-p))(\ln(1/\beta) + d)$.

As pointed out in Schildbach et al. [19], a drawback to this random generation of scenarios is that some may be far from the reality of the process, and consequently, the optimal controls calculated can cause erroneous behaviour in the closed-loop system. To improve the cost function while $\mathbb{P}[x_{i+1|k} \in \mathbb{X}] \geq p$ holds for a sufficiently high number of M generated scenarios, D scenarios can be discarded [35] from the total of M scenarios constraints where D is the maximum value that meets

$$\binom{D+d-1}{D} \sum_{j=0}^{D+d-1} \binom{M}{j} (1-p)^j p^{M-j} \leq \beta. \tag{7}$$

In [19], a sample-removal pair is proposed and consists of calculating the pair (M, D) based in a defined risk acceptability level of constraint violation $(1-p)$ such that $\mathbb{P}[x_{i+1|k} \in \mathbb{X}] \geq p$, where M is the number of scenarios to be considered in the OCP, D is the number of scenarios that can be discarded from the constraints in the states and ρ is a parameter related to the dimension of the unconstrained subspace of the search space \mathbb{R}^d

$$\int_0^1 U(v) dv \leq 1-p \tag{8}$$

$$U(v) = \min \left\{ 1, \binom{D+\rho-1}{D} \sum_{j=0}^{D+\rho-1} \binom{M}{j} v^j (1-v)^{M-j} \right\}.$$

The use of these scenario removal schemes represents an increase in the solution time, which could result in an OCP that is expensive to solve computationally. This is because of the need for large values for M to continue fulfilling $\mathbb{P}[x_{i+1|k} \in \mathbb{X}] \geq p$ with the remaining $M - D$ scenarios; in addition to requiring an appropriate algorithm [19,35] to identify unlikely scenarios to be removed from the constraints to reduce conservatism.

3. Model predictive control via conditional scenarios

In this section, a novel scenario-based MPC approach is presented. At each sampling time, a primary set of equiprobable scenarios is generated and is subsequently approximated to a reduced set of conditional scenarios, each with its probability of occurrence. This reduced set is used to solve an OCP whose structure is similar to that of a scenario-based MPC Eq. (5), but considers a new cost function in which the predicted states and inputs are penalised according to the probabilities of occurrence associated with the realisations of the uncertainties on which they depend.

3.1. Conditional scenario approach

The conditional scenario (CS) concept was presented in Beltran-Royo [49] as an approximation to the two-stage stochastic mixed-integer linear programming (SMILP) problem, where

the expected value of the second stage cost is commonly stated in terms of scenarios defined as realisations of a random vector $\delta = [\xi_1, \xi_2, \dots, \xi_{n_\delta}]^\top$. In this method such realisations are made assuming that δ has a known multivariate normal distribution and bounded support, resulting in a set of so-called conditional scenarios, each with its respective probability of occurrence.

The aforementioned CS approach was adapted in Beltran-Royo [50] as a scenario reduction method for a given large primary set $\{\tilde{\delta}^{[1]}, \tilde{\delta}^{[2]}, \dots, \tilde{\delta}^{[S]}\} \in \mathbb{S}$ of scenarios, whose l th scenario and its probability are $\tilde{\delta}^{[l]} = [\tilde{\xi}_1^{[l]}, \tilde{\xi}_2^{[l]}, \dots, \tilde{\xi}_{n_\delta}^{[l]}]^\top$ and $\tilde{p}^{[l]}$, respectively, $\forall l \in \{1, 2, \dots, S\}$. Such reduction is made based on \mathbb{S} and a desired number of points E to discretise the support of each random variable $\tilde{\xi}$, and leading to a new set of C conditional scenarios $\{\hat{\delta}^{[1]}, \hat{\delta}^{[2]}, \dots, \hat{\delta}^{[C]}\} \in \mathbb{S}_C$, each one $\hat{\delta}^{[j]} = [\hat{\xi}_1^{[j]}, \hat{\xi}_2^{[j]}, \dots, \hat{\xi}_{n_\delta}^{[j]}]^\top$ with its own probability of occurrence $\hat{p}^{[j]} \forall j \in \{1, 2, \dots, C\}$. The methodology of Beltran-Royo [51,52] for the reduction of a primary set through the CS approach is described in Algorithm 1, and in which the

Algorithm 1 Conditional scenario reduction method.

Input: the primary set of scenarios $\{\tilde{\delta}^{[1]}, \tilde{\delta}^{[2]}, \dots, \tilde{\delta}^{[S]}\}$, their probability levels $\{\tilde{p}^{[1]}, \tilde{p}^{[2]}, \dots, \tilde{p}^{[S]}\}$ and a desired integer value for E .

Output: the new set of C conditional scenarios $\{\hat{\delta}^{[1]}, \hat{\delta}^{[2]}, \dots, \hat{\delta}^{[C]}\}$ and their respective probability levels $\{\hat{p}^{[1]}, \hat{p}^{[2]}, \dots, \hat{p}^{[C]}\}$, where $C = n_\delta E$.

Procedure:

1: For each random variable $\tilde{\xi}_n \forall n \in \{1, 2, \dots, n_\delta\}$ obtain its extreme values $I_n = [a_n, b_n]$ in which

$$a_n = \min\{\tilde{\xi}_n^{[1]}, \tilde{\xi}_n^{[2]}, \dots, \tilde{\xi}_n^{[S]}\}, \quad b_n = \max\{\tilde{\xi}_n^{[1]}, \tilde{\xi}_n^{[2]}, \dots, \tilde{\xi}_n^{[S]}\}$$

2: Split every I_n into E subintervals $I_{n,e}$ of equal or different lengths such that $I_n = \bigcup_{e=1}^E I_{n,e} \forall e \in \{1, 2, \dots, E\}$ and $\{I_{n,1}, I_{n,2}, \dots, I_{n,E}\} = \{[a_n, b_{n,1}), [b_{n,1}, b_{n,2}), \dots, [b_{n,(E-1)}, b_n]\}$.

3: For each $I_{n,e}$, construct the sets $\{\tilde{\delta}_{n,e}^{[1]}, \tilde{\delta}_{n,e}^{[2]}, \dots, \tilde{\delta}_{n,e}^{[S_n]}\}$, $\{\tilde{p}_{n,e}^{[1]}, \tilde{p}_{n,e}^{[2]}, \dots, \tilde{p}_{n,e}^{[S_n]}\}$ with every pair $(\tilde{\delta}^{[l]}, \tilde{p}^{[l]}) \forall l \in \{1, 2, \dots, S\}$ that meet the condition $\tilde{\xi}_n^{[l]} \in I_{n,e}$ and compute its respective CS $\hat{\delta}^{[n,e]}$ with probability level $\hat{p}^{[n,e]}$

$$\hat{\delta}^{[n,e]} = \mathbb{E}[\tilde{\delta} \mid \tilde{\xi}_n \in I_{n,e}] = \frac{1}{S_n} \sum_{j=1}^{S_n} \tilde{\delta}_{n,e}^{[j]}, \quad \hat{p}^{[n,e]} = \frac{1}{n_\delta} \sum_{j=1}^{S_n} \tilde{p}_{n,e}^{[j]}$$

number of reduced scenarios is $C = n_\delta E$, provided that at least one scenario of \mathbb{S} fulfills the condition $\tilde{\xi}_n^{[l]} \in I_{n,e}$. As can be seen in step 3, this approach, rather than filtering or reducing scenarios, performs an approximation of \mathbb{S} to a set of conditional expectations.

In [52] and [50], comparisons were made of the performance of this reduction technique and two others (such as sample average approximation (SAA) [53] and scenario reduction based on probability distances (SRD) [54]) to solve portfolio optimisation and capacitated facility location problems. These three techniques yielded similar results, but with less time dedicated to the reduction by the CS (up to eight times faster).

3.2. Formulation of conditional scenarios in MPC

In the following, a procedure that adapts the CS reduction approach to the scenario-based MPC framework is proposed. As a remark, a scenario in the SMILP context consists of a realisation of the random vector δ (with cardinality n_δ), while in the scenario-based MPC context this consists of a sequence of N realisations of δ represented by $\Delta_k = \{\delta_{0|k}, \delta_{1|k}, \dots, \delta_{N-1|k}\}$. In line with the above, let \mathbb{S}_S be a set (with cardinality S) of random scenarios generated at time k

$$\{\Delta_k^{[1]}, \Delta_k^{[2]}, \dots, \Delta_k^{[S]}\} \in \mathbb{S}_S \tag{9}$$

$$\Delta_k^{[l]} = \{\delta_{0|k}^{[l]}, \delta_{1|k}^{[l]}, \dots, \delta_{N-1|k}^{[l]}\}, \quad \forall l \in \{1, 2, \dots, S\}$$

where \mathbb{S}_S is assumed to be a set of equiprobable scenarios, that is, $\Delta_k^{[l]}$ has a probability of occurrence $p = 1/S$. Hence, each element of $\{\delta_{i|k}^{[1]}, \delta_{i|k}^{[2]}, \dots, \delta_{i|k}^{[S]}\}$ has a probability $p_{i|k}^{[l]} = 1/S$

$$\{p_k^{[1]}, p_k^{[2]}, \dots, p_k^{[S]}\}, \quad p_k^{[l]} = \{p_{0|k}^{[l]}, p_{1|k}^{[l]}, \dots, p_{N-1|k}^{[l]}\}$$

$$p_{i|k}^{[l]} = 1/S, \quad \forall i \in \{0, 1, \dots, N - 1\}.$$

Based on Algorithm 1, the proposed procedure to approximate a set of equiprobable scenarios \mathbb{S}_S Eq. (9) to a reduced set of conditional scenarios \mathbb{S}_C Eq. (10a), with probabilities of occurrence Eq. (10b) (where $\sum_{j=1}^C \hat{p}_{i|k}^{[j]} = 1$), in the context of scenario-based MPC is summarised in Algorithm 2. To do this, the integers C (number of desired CSs) and E (number of subintervals) must first be defined taking into account that they must satisfy the condition $C = n_\delta E$

$$\{\hat{\Delta}_k^{[1]}, \hat{\Delta}_k^{[2]}, \dots, \hat{\Delta}_k^{[C]}\} \in \mathbb{S}_C \tag{10a}$$

$$\{\hat{p}_k^{[1]}, \hat{p}_k^{[2]}, \dots, \hat{p}_k^{[C]}\} \tag{10b}$$

$$\hat{\Delta}_k^{[j]} = \{\hat{\delta}_{0|k}^{[j]}, \hat{\delta}_{1|k}^{[j]}, \dots, \hat{\delta}_{N-1|k}^{[j]}\}, \quad \hat{p}_k^{[j]} = \{\hat{p}_{0|k}^{[j]}, \hat{p}_{1|k}^{[j]}, \dots, \hat{p}_{N-1|k}^{[j]}\}, \quad \forall j \in \{1, 2, \dots, C\}.$$

The implementation of this procedure is straightforward, since Algorithm 2 does not require an optimisation stage or knowledge about how the random variables are distributed to perform the reduction.

Assumption 3. Scenario Generation and Reduction: Defining the integers C and E such that $C = n_\delta E$. At every control period, a new primary set of equiprobable scenarios \mathbb{S}_S is generated in accordance with Assumption 1 and is later approximated to the CSs reduced set \mathbb{S}_C applying the steps of Algorithm 2.

To illustrate how Algorithm 2 works, Fig. 1(a) shows a primary set \mathbb{S}_S of 500 scenarios for a prediction horizon $N = 3$, considering a random vector $\delta = [\xi_1, \xi_2]^T$ with multivariate normal distribution $\delta \sim \mathcal{N}_2(\mu, \Sigma)$, mean $\mu = [0, 0]^T$, covariance $\Sigma = \begin{bmatrix} 1.0 & 0.8 \\ 0.8 & 1.0 \end{bmatrix}$ and bounds $|\delta| \leq [2, 2]^T$. By setting $E = 7$, a new set \mathbb{S}_C of 14 CSs is obtained. For both \mathbb{S}_S and \mathbb{S}_C , the elements $\delta_{i|k}^{[l]}$ of $\Delta_k^{[l]}$, and $\hat{\delta}_{i|k}^{[j]}$ of $\hat{\Delta}_k^{[j]}$ are plotted on its corresponding $i|k$ -step graph. As illustrated in Fig. 1(b), every approximation $\hat{\delta}_{i|k}^{[j]}$ belonging to each CS, has a probability of

Algorithm 2 From scenarios to conditional scenarios in MPC.

Input: the primary set of equiprobable scenarios Eq. (9) and a desired integer E such that $C = n_\delta E$.

Output: the new set of CSs $\{\hat{\Delta}_k^{[1]}, \hat{\Delta}_k^{[2]}, \dots, \hat{\Delta}_k^{[C]}\}$ and their respective probabilities sequences $\{\hat{p}_k^{[1]}, \hat{p}_k^{[2]}, \dots, \hat{p}_k^{[C]}\}$.

Procedure:

1: Classify all the realisations of the uncertainties into N groups δ_i and $p_i \forall i \in \{0, 1, \dots, N - 1\}$, with cardinality S so that each pair corresponds to the i th prediction step

$$\delta_i = \{\delta_{i|k}^{[1]}, \delta_{i|k}^{[2]}, \dots, \delta_{i|k}^{[S]}\}, \quad p_i = \{p_{i|k}^{[1]}, p_{i|k}^{[2]}, \dots, p_{i|k}^{[S]}\}, \quad p_{i|k}^{[-]} = 1/S$$

2: Apply Algorithm 1 to each pair (δ_i, p_i) to obtain $\hat{\delta}_i^{[n,e]}$ and its probability $\hat{p}_i^{[n,e]}$, $\forall n \in \{1, 2, \dots, n_\delta\} \forall e \in \{1, 2, \dots, E\}$

3: Construct the new reduced set $\hat{\delta}_i = \{\hat{\delta}_{i|k}^{[1]}, \hat{\delta}_{i|k}^{[2]}, \dots, \hat{\delta}_{i|k}^{[C]}\}$ and its probabilities $\hat{p}_i = \{\hat{p}_{i|k}^{[1]}, \hat{p}_{i|k}^{[2]}, \dots, \hat{p}_{i|k}^{[C]}\}$

$$\hat{\delta}_i = \{\hat{\delta}_i^{[1,1]}, \dots, \hat{\delta}_i^{[1,E]}, \dots, \hat{\delta}_i^{[n_\delta,1]}, \dots, \hat{\delta}_i^{[n_\delta,E]}\}$$

$$\hat{p}_i = \{\hat{p}_i^{[1,1]}, \dots, \hat{p}_i^{[1,E]}, \dots, \hat{p}_i^{[n_\delta,1]}, \dots, \hat{p}_i^{[n_\delta,E]}\}$$

4: Randomly rearrange the $\hat{\delta}_i$ and \hat{p}_i sequences ensuring that any pair $(\hat{\delta}_{i|k}^{[j]}, \hat{p}_{i|k}^{[j]}) \forall j \in \{1, 2, \dots, C\}$ share the same positions.

5: Construct j th conditional scenario $\hat{\Delta}_k^{[j]}$ and its respective sequence of probabilities $\hat{p}_k^{[j]}$

$$\hat{\Delta}_k^{[j]} = \{\hat{\delta}_{0|k}^{[j]}, \hat{\delta}_{1|k}^{[j]}, \dots, \hat{\delta}_{N-1|k}^{[j]}\}, \quad \hat{p}_k^{[j]} = \{\hat{p}_{0|k}^{[j]}, \hat{p}_{1|k}^{[j]}, \dots, \hat{p}_{N-1|k}^{[j]}\}$$

6: Group them such that

$$\{\hat{\Delta}_k^{[1]}, \hat{\Delta}_k^{[2]}, \dots, \hat{\Delta}_k^{[C]}\}, \quad \{\hat{p}_k^{[1]}, \hat{p}_k^{[2]}, \dots, \hat{p}_k^{[C]}\}$$

occurrence in accordance with the number of primary scenarios surrounding it. Considering the first CS (coloured yellow), its values are $\hat{\Delta}_k^{[1]} = \left\{ \begin{bmatrix} 0.0553 \\ -0.0085 \end{bmatrix}, \begin{bmatrix} 0.5295 \\ 0.4130 \end{bmatrix}, \begin{bmatrix} -1.0872 \\ -0.8625 \end{bmatrix} \right\}$ with $\hat{p}_k^{[1]} = \{0.118, 0.109, 0.062\}$.

3.3. Cost function and control problem

As mentioned in the previous section, two of the most important drawbacks in scenario-based MPC are the unlikely scenarios that could cause undesired behaviour in the closed-loop system, and the computational tractability when the number of scenarios to be considered is large. For this reason, an approximation of the primary set of equiprobable scenarios to a set of conditional scenarios is suitable since it would allow addressing both the drawbacks mentioned above.

Given current instant k and according to Assumption 3, consider \mathbb{S}_S the primary set of generated scenarios Eq. (9) for N steps, whose subsequent approximation through Algorithm 2 produces the new reduced set \mathbb{S}_C given by Eq. (10). The value of C can be

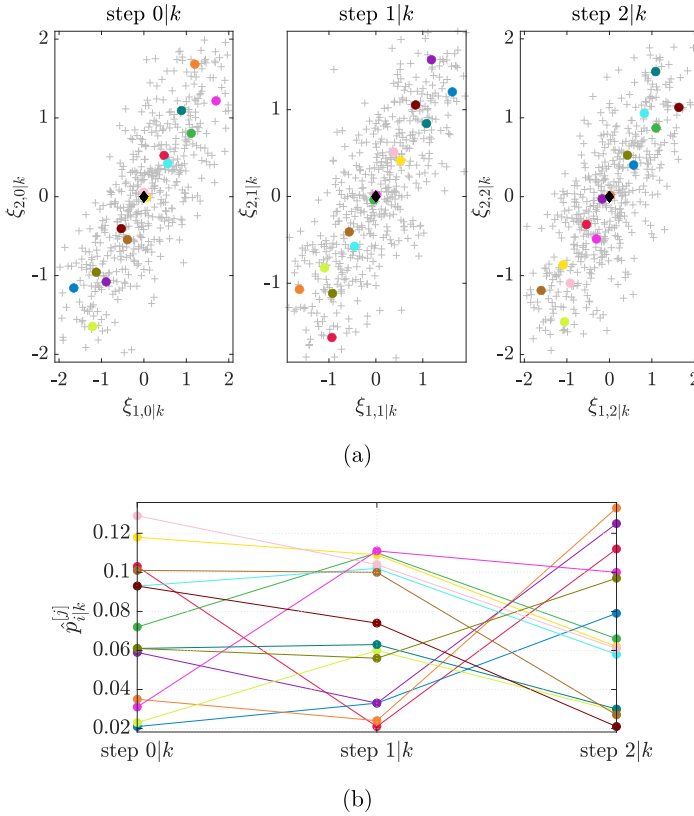


Fig. 1. Illustrative example of Algorithm 2. (a) The primary set \mathbb{S}_S of 500 equiprobable scenarios (plus signs) for a prediction horizon $N = 3$, the new reduced set \mathbb{S}_C of 14 CSs (each with their respective single-coloured dots), and the origin (black rhombus). (b) Probabilities of occurrence of the $\hat{\delta}_{i|k}^{[j]}$ of each scenario at each time-step.

defined according to any criterion, e.g., Eqs. (6)–(8). In the case of using one of the last two mentioned schemes, the scenarios to be removed from the constraints are those with the lowest probability of occurrence.

Evaluating Eqs. (4a) and (4b) with Eq. (10a), produces the predictions of the states and inputs for such reduced scenarios, which are then incorporated in the cost function given by

$$\hat{J}_{CS}(\hat{x}_k, \mathbf{v}_k) = \frac{1}{C} \sum_{j=1}^C \left[\sum_{i=0}^{N-1} \left(\hat{p}_{i-1|k}^{[j]} \|x_{i|k}^{[j]}\|_Q^2 + \hat{p}_{i|k}^{[j]} \|u_{i|k}^{[j]}\|_R^2 \right) + \hat{p}_{N-1|k}^{[j]} \|x_{N|k}^{[j]}\|_P^2 \right]. \tag{11}$$

This new function, in addition to taking into account the terms $x_{i|k}^{[j]}$ and $u_{i|k}^{[j]}$, also includes the set of probabilities Eq. (10b) as weights. This means that, the predicted state $x_{i|k}^{[j]}$ and input $u_{i|k}^{[j]}$, which depends on the realisations $\hat{\delta}_{i-1|k}^{[j]}$ and $\hat{\delta}_{i|k}^{[j]}$, respectively, are penalised with the probability of occurrence $\hat{p}_{i-1|k}^{[j]}$ and $\hat{p}_{i|k}^{[j]}$ that are associated with such a realisation, where $\hat{p}_{-1|k}^{[j]} = 1/C$ since $x_{0|k}^{[j]} = \hat{x}_k$.

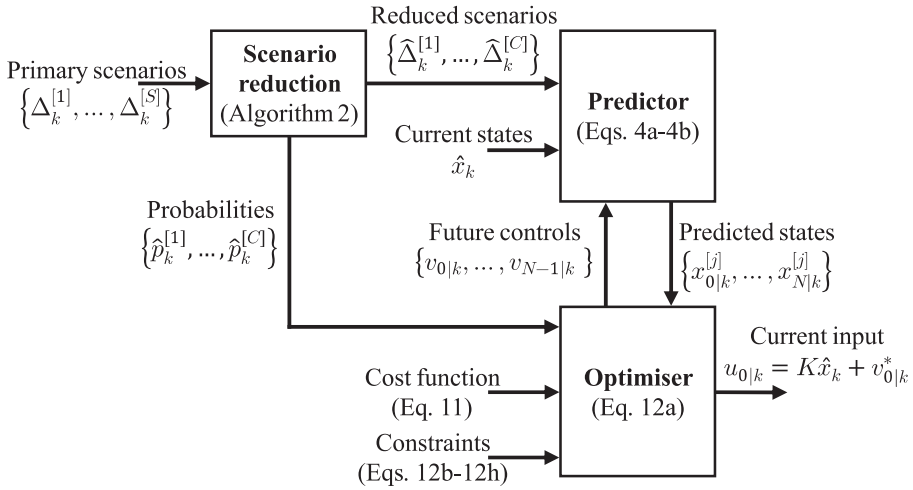


Fig. 2. Block diagram of CSB-MPC.

Thus, the control problem to be solved in the context of conditional scenario-based model predictive control (CSB-MPC) is stated in Eq. (12). In addition, in Fig. 2 the schematic diagram of its operation is depicted

$$\min_{v_{0|k}, v_{1|k}, \dots, v_{N-1|k}} \hat{J}_{CS}(\hat{x}_k, \mathbf{v}_k) \tag{12a}$$

s.t.

$$x_{i+1|k}^{[j]} = A(\hat{\delta}_{i|k}^{[j]})x_{i|k}^{[j]} + B(\hat{\delta}_{i|k}^{[j]})u_{i|k}^{[j]} + Gw(\hat{\delta}_{i|k}^{[j]}) \tag{12b}$$

$$u_{i|k}^{[j]} = Kx_{i|k}^{[j]} + v_{i|k} \tag{12c}$$

$$x_{i+1|k}^{[j]} \in \mathbb{X} \tag{12d}$$

$$u_{i|k}^{[j]} \in \mathbb{U} \tag{12e}$$

$$x_{N|k}^{[j]} \in \mathbb{X}_T \tag{12f}$$

$$x_{0|k}^{[j]} = \hat{x}_k, \quad \hat{p}_{-1|k}^{[j]} = 1/C \tag{12g}$$

$$\forall i \in \{0, 1, \dots, N - 1\}, \quad \forall j \in \{1, 2, \dots, C\} \tag{12h}$$

As can be seen, the structure of Eq. (12) is similar to that of Eq. (5), but with the difference that this new structure is based on a reduced set \mathbb{S}_C , obtained through the reduction stage, and the new cost function Eq. (11).

The OCP Eq. (12) covers the topic related to unlikely scenarios by giving more relevance to the states and inputs that involve realisations with more probability of occurrence, and less importance given to those that are related to unlikely realisations, by means of their associated probabilities. Likewise, according to Theorem 3.1 in Calafiore [43] and Theorem 2.1 in Campi and Garatti [35], it holds that any optimal solution v_k^* obtained by the scenario program Eq. (12), using C conditional scenarios, with C defined using either Eqs. (6) and (7), has a guaranteed level $1 - \beta$ of feasibility, in a probabilistic sense, of meeting the probabilistic constraints $\mathbb{P}[x_{i+1|k} \in \mathbb{X}] \geq p$.

On the other hand, if solving Eq. (12) for C conditional scenarios presents better the probability of constraints satisfaction, compared to solving Eq. (5) for C random equiprobable scenarios, the topic related to computational tractability can be improved using a CSB-MPC with a number of conditional scenarios smaller than C .

Recursive feasibility and stability in MPC is to ensure that the OCP is always feasible and that the system states, over time, converge asymptotically to a desired operating point. Based on the dual paradigm, recursive feasibility and stability are obtained through the terminal cost $\|x_N\|_p^2$, the terminal set \mathbb{X}_T and additional conditions [42,45]. If the initial state x_0 belongs to the feasible set $\mathbb{X}_f \subset \mathbb{X}$, there will exist a parametrised control law $u_i = Kx_i + v_i$ ($\forall i \in \{0, 1, \dots, N-1\}$), whereby the states converge asymptotically to the origin, such that $x_N \in \mathbb{X}_T$. For instants from N , the system is governed by the law $u_i = Kx_i$ ($\forall i \in \{N, N+1, \dots\}$), for which \mathbb{X}_T is positively invariant, ensuring that the OCP is feasible indefinitely.

In a Scenario-based MPC in the current form of Eqs. (5) and (12), recursive feasibility and stability remains a subject of research. This is because Eq. (1a) considers both parametric and additive uncertainties, with a δ of stochastic nature, where all elements of the sequence of uncertainties $\{\delta_0, \delta_1, \dots\}$ are assumed to be independent and identically distributed (i.i.d.), i.e., independent in time; and whose δ characteristics can be time-varying in nature. An unbounded δ can produce realisations with very large values of the uncertainties, making the OCP unable to find a solution that satisfies the constraints, while a bounded δ , as proposed in this work and as is the case in most real processes, prevents these large and unlikely realisations from appearing, besides allowing the calculation of an appropriate cost $\|x_N\|_p^2$ and a robust invariant set \mathbb{X}_T to be obtained.

A practical way to ensure that the OCP Eq. (12) is always feasible is by introducing slack variables that soften the constraints [18,20]. These new decision variables are incorporated and penalised in the cost function to force their values to be zero if an optimum solution can be obtained without violating the softened constraints.

On the other hand, a combination (through Algorithm 2 to extract the most representative scenarios of \mathbb{S}_S) with approaches based on offline uncertainty sampling [12,16,17,26] (which in general use either Eqs. (6) and (7)) can be used to guarantee the recursive feasibility and stability of Eq. (12) but require that the characteristics of the uncertainties (mean, covariance, bounds) remain invariant, thus missing the attractiveness of the approach, which is the possibility to include new uncertainty data online, which may be the case for several processes. For example, in Lorenzen et al. [12], a first-step constraint \mathbb{D}_R and a terminal set \mathbb{X}_T are proposed, considering that Eq. (1a) has only parametric uncertainties, bounded and with i.i.d. sequences. In [26], a constraint for MPC initialisation, and a terminal robust invariant set \mathbb{X}_T are proposed employing probabilistic reachable sets (PRS), considering that Eq. (1a) has

only additive uncertainties, whose sequences are time-correlated (non-i.i.d.) and possibly unbounded. In [17], a system Eq. (1a) with only additive and unbounded uncertainties with i.i.d. sequences is considered. As in Hewing and Zeilinger [26], it uses PRS to address probabilistic constraints; feasibility and stability are addressed by incorporating slack variables in the initial state constraints (called therein as flexible initial state constraint) and a robustly invariant terminal set, respectively.

In this work, in order to maintain the classical formulation of a scenario-based MPC, the feasibility of the OCP at each time-step is assumed according to Assumption 2.

4. Numerical examples

In this section, two numerical examples are presented to illustrate and compare the behaviour of a scenario-based MPC Eq. (5) and a CSB-MPC Eq. (12) for $N_r = 1000$ Monte Carlo simulations each. In both techniques, at each control period, a primary set \mathbb{S}_S of scenarios is generated where the OCP Eq. (5) in the scenario-based MPC (for simplicity, hereafter referred to as ScMPC) is solved by considering M scenarios taken randomly from \mathbb{S}_S . The CSB-MPC Eq. (12) is solved for C conditional scenarios obtained from the reduction of \mathbb{S}_S by applying Algorithm 2. In each simulation, the purpose of each MPC strategy is to control the system and steer its states from the initial point $x_{0|k}^{l|j} = \hat{x}_0$ to the origin (assuming that the current state is measurable).

All N_r simulations were carried out using Matlab R2018b, installed on a standard computer and the control actions were calculated with the quadprog toolbox [55] available in the Mosek 9.2. optimisation software. Through a stability analysis of Lyapunov's [7,48], K and P matrices were computed using YALMIP [56] to solve a problem based on linear matrix inequalities; and the robust invariant set \mathbb{X}_T , consisting of a polytope, was computed using the multi-parametric toolbox (MPT) [57]. Readers can reproduce the simulation results here presented or simulate an CSB-MPC with the specialised software *conditional scenario-based MPC toolbox* as developed by the authors and available in MATLAB Central [58].

The behaviour of both MPC strategies is analysed by means of performance indices, which were computed based on the N_r closed-loop state responses and inputs. These are:

- $p_s = 100(N_s/N_r)$: probability (in percentage) of success of a simulation, where N_s is the number of simulations out of all N_r where no constraints were violated.
- p_c : the minimum probability (in percentage) that all states do not violate the constraints.
- N_v : the total number of constraints that were violated in all simulations.
- PD_{avg} : average percentage of deviation of violated constraints in the states.
- IAE_{avg} : mean value of the integral absolute error of all states.
- IAU_{avg} : mean value of the integral of the absolute value of the applied inputs.
- t_{avg} : average time taken by the MPC algorithm to obtain a solution. For ScMPC and CSB-MPC, this time also includes the times it takes to generate the primary set \mathbb{S}_S , plus select M or approximate to C scenarios, depending on the case.

4.1. Example 1

Consider the second order discrete system in the form Eq. (1a), given by

$$x_{i+1} = \begin{bmatrix} 1 & 0.93 \\ 0 & 1 \end{bmatrix} x_i + \begin{bmatrix} 0.28 \\ 0.82 \end{bmatrix} u_i + \begin{bmatrix} 1 & 0 \\ 0 & 1 \end{bmatrix} w(\delta_i).$$

Table 1
Performance indices of the MPCs in Example 1 for a \mathbb{S}_S of 5000 scenarios.

Controller	p_s	p_c	N_v	PD _{avg}	IAE _{avg}	IAU _{avg}	t_{avg}
ScMPC ₁₀₀	92.8%	98.8%	74	1.22%	69.054	4.239	22.0 ms
CSB-MPC ₁₀₀	98.1%	99.6%	19	0.20%	69.554	4.198	43.8 ms
ScMPC ₈₀	91.0%	98.6%	93	1.34%	68.925	4.251	19.1 ms
CSB-MPC ₈₀	97.7%	99.6%	23	0.26%	69.492	4.201	38.2 ms
ScMPC ₆₀	87.8%	98.0%	127	1.53%	68.728	4.268	16.3 ms
CSB-MPC ₆₀	96.9%	99.3%	31	0.35%	69.399	4.207	31.7 ms
ScMPC ₄₀	81.4%	96.5%	201	1.88%	68.387	4.300	13.1 ms
CSB-MPC ₄₀	95.1%	99.1%	49	0.52%	69.216	4.217	25.0 ms
ScMPC ₂₀	63.9%	94.6%	424	2.81%	67.643	4.390	10.1 ms
CSB-MPC ₂₀	87.7%	98.2%	131	0.98%	68.649	4.250	18.3 ms

The sampling time is $T_s = 0.5$ s, the system state and input constraints are $|x_2| \leq 1$ for the second state and $|u| \leq 0.8$, respectively. The two random variables, ξ_1 and ξ_2 , contained in the vector of additive disturbances $w(\delta_i) = [\xi_{1,i}, \xi_{2,i}]^T$ make up the random vector $\delta = [\xi_1, \xi_2]^T$ ($n_\delta = 2$), which has a truncated multivariate normal distribution $\delta \sim \mathcal{N}_2(\mu, \Sigma)$ with bounds $|\delta| \leq [0.05, 0.2]^T$; and a mean vector $\mu = [0, 0]^T$ and covariance matrix $\Sigma = \begin{bmatrix} 0.0004 & 0.0017 \\ 0.0017 & 0.01 \end{bmatrix}$.

4.1.1. Simulation setup

The performances in this example of a ScMPC and a CSB-MPC for various $M, C = \{100, 80, 60, 40, 20\}$ used to solve the OCP are compared for the cases of primary sets \mathbb{S}_S , consisting of 5000 and 1200 scenarios. All elements in this sequence meet the condition $C = n_\delta E$ (see Assumption 3), and through Eq. (6), with $\beta = 10^{-9}$, their theoretical probabilities of constraints satisfaction $\mathbb{P}[x_{i+1} \in \mathbb{X}] \geq p_t$ are $p_t(M, C) = \{57.5\%, 49.5\%, 37.5\%, 20.2\%, 0.52\%\}$. The duration of each of the N_r simulations in both MPCs is 20 sampling periods, starting from the initial state $x_{0|k}^{[j]} = \hat{x}_0 = [8, 0.7]^T$. The prediction horizon is $N = 15$, the cost function weights are $Q = \text{diag}(1, 1)$ and $R = 0.1$; the terminal set \mathbb{X}_T consisting of a polytope of 6 linear inequalities and K and P matrices are $K = [-0.7421 \quad -1.5891]$ and $P = \begin{bmatrix} 2.3026 & 0.8572 \\ 0.8572 & 1.6983 \end{bmatrix}$, respectively.

4.1.2. Results

Tables 1 and 2 show the performance results of each MPC for the primary sets $\mathbb{S}_S(5000)$ and $\mathbb{S}_S(1200)$, respectively. The first column corresponds to the type of controller, whose subscript indicates the number of scenarios used to solve its respective OCP. The subsequent columns indicate the performance indices, as defined at the beginning of this section and which were computed based on the N_r closed-loop responses. Furthermore, these indices are depicted in Fig. 3(a) and (b), in which the orange and blue lines represent those in Tables 1 and 2, respectively.

Both tables reveal that for the two cases of \mathbb{S}_S primary sets, CSB-MPCs obtained higher constraint satisfaction probabilities p_s and p_c than ScMPCs; where, according to Fig. 3(a) a greater difference is noted as the number of scenarios decreases. Likewise, it is verified

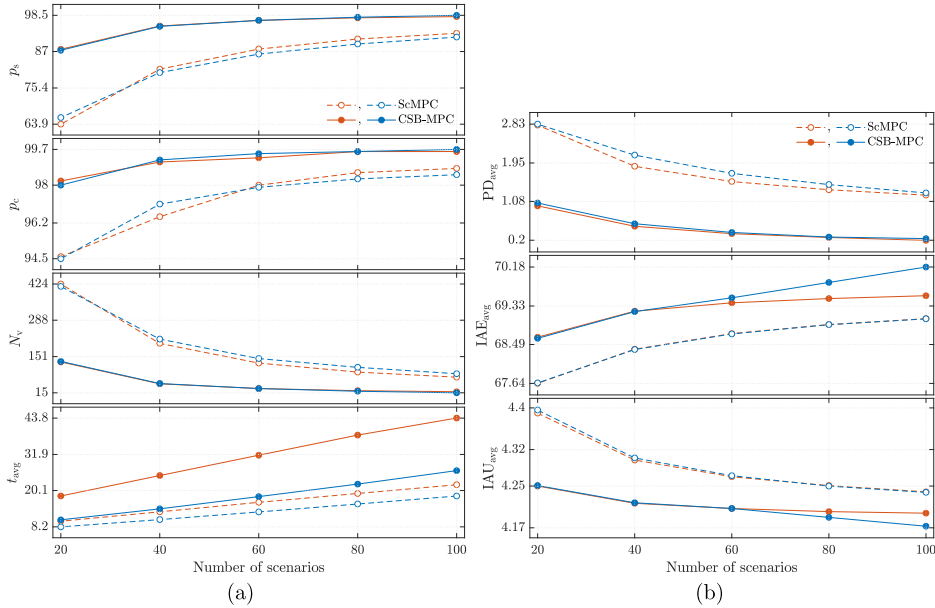


Fig. 3. Graphs of the performance indices from Tables 1 ($\mathbb{S}_S(5000)$, orange lines) and 2 ($\mathbb{S}_S(1200)$, blue lines), corresponding to ScMPC (dashed lines) and CSB-MPC (solid lines), for 20, 40, 60, 80 and 100 scenarios. (For interpretation of the references to colour in this figure legend, the reader is referred to the web version of this article.)

Table 2
Performance indices of the MPCs in Example 1 for a \mathbb{S}_S of 1200 scenarios.

Controller	p_s	p_c	N_v	PD_{avg}	IAE_{avg}	IAU_{avg}	t_{avg}
ScMPC ₁₀₀	91.6%	98.5%	87	1.27%	69.051	4.238	18.3 ms
CSB-MPC ₁₀₀	98.5%	99.7%	15	0.24%	70.180	4.173	26.6 ms
ScMPC ₈₀	89.4%	98.3%	111	1.46%	68.924	4.250	15.7 ms
CSB-MPC ₈₀	97.9%	99.6%	21	0.27%	69.843	4.190	22.2 ms
ScMPC ₆₀	86.2%	97.9%	144	1.72%	68.721	4.270	13.1 ms
CSB-MPC ₆₀	96.9%	99.5%	31	0.38%	69.509	4.207	18.1 ms
ScMPC ₄₀	80.3%	97.1%	217	2.13%	68.380	4.304	10.6 ms
CSB-MPC ₄₀	95.0%	99.2%	50	0.57%	69.207	4.218	14.1 ms
ScMPC ₂₀	66.0%	94.5%	415	2.83%	67.652	4.396	8.2 ms
CSB-MPC ₂₀	87.4%	98.0%	133	1.04%	68.624	4.251	10.5 ms

that the empirical probabilities p_s of the CSB-MPCs satisfy the theoretical probabilities p_t , presenting values significantly above the estimated ones.

Moreover, this improvement in the probability of constraint satisfaction by CSB-MPCs produces lower numbers of violated constraints N_v and lower percentages of deviations from constraints PD_{avg} than ScMPCs, being almost one-third of those reported by ScMPCs (e.g., ScMPC₂₀ and CSB-MPC₂₀ in Table 1). In addition, Fig. 4 shows the closed-loop state trajectories and applied inputs for $M, C = 20$ in Table 2, contrasted with those of a standard MPC with constraints (in which $p_s = 0.1\%$ and $p_c = 46.5\%$) that is based on the nominal

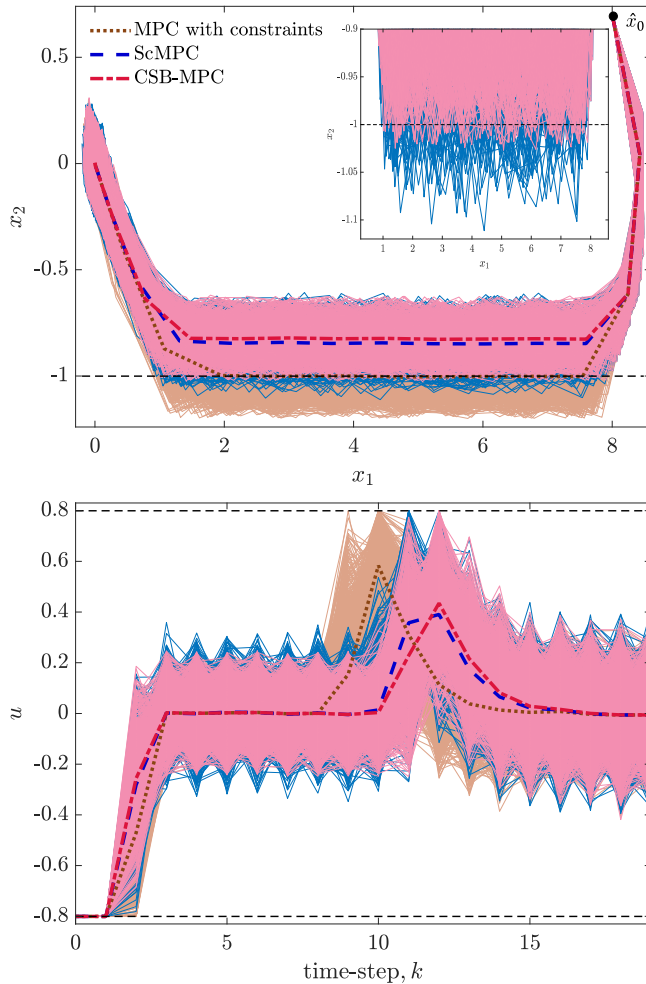


Fig. 4. 1000 system closed-loop responses and applied inputs to a standard MPC with constraints (light brown solid lines), ScMPC₂₀ (light blue solid lines) and CSB-MPC₂₀ (light red solid lines) controllers, for a \mathbb{S}_S of 1200 Scenarios. The brown dotted line, blue dashed line, and red dash-dotted line represent the mean trajectories of standard MPC, ScMPC and CSB-MPC, respectively; and the system constraints, $|x_2| \leq 1.0$, $|u| \leq 0.8$, represented by black dashed lines. (For interpretation of the references to colour in this figure legend, the reader is referred to the web version of this article.)

model of the system. As can be seen in the detailed view, the state trajectories of the ScMPC ($N_v = 415$, $PD_{avg} = 2.83\%$) transgress the limits, more times than those of the CSB-MPC ($N_v = 133$, $PD_{avg} = 1.04\%$), which has better probabilities p_s and p_c .

Note that for both primary sets $\mathbb{S}_S = 5000$ and $\mathbb{S}_S = 1200$ (see Fig. 3), the CSB-MPC do not show considerable variations in indicators p_s , p_c , N_v and PD_{avg} , as is the case for indicator t_{avg} , which decreases with $\mathbb{S}_S(1200)$, approaching those of the ScMPC. This decrease in t_{avg} is because the time used in the additional scenario-reduction stage of the CSB-MPC, is less as the primary set to approximate is smaller. With this in mind and with an appropriately sized \mathbb{S}_S , a CSB-MPC against a ScMPC with the same number of scenarios is a good option

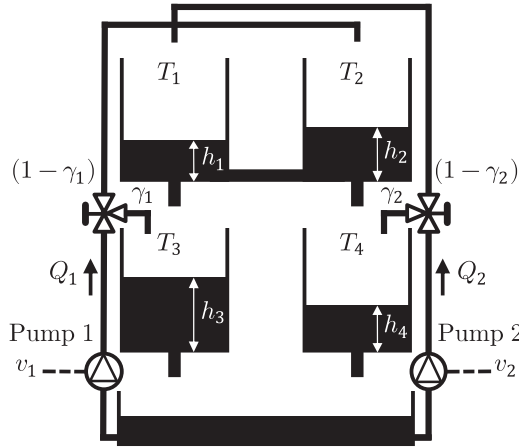


Fig. 5. Quadruple tank process schematic diagram.

due to its higher probabilistic feasibility of constraints satisfaction, with similar solution times t_{avg} . Furthermore, in case of needing a decrease in the solution time t_{avg} , a CSB-MPC with a smaller number of scenarios than a ScMPC could be used. For example, considering the MPCs in Table 2, if similar performance indices to those of the ScMPC₁₀₀ ($t_{avg} = 18.3$ ms) are required, but with a lower solution time, the CSB-MPC₆₀ ($t_{avg} = 18.1$ ms) or CSB-MPC₄₀ ($t_{avg} = 14.1$ ms) could be used. Note that the others ScMPCs reported in Table 2 do not offer similar or superior characteristics to those required, as do the mentioned CSB-MPCs, which even offer higher probabilities, lower violated constraints N_v and lower PD_{avg} .

Regarding indicators IAE_{avg} and IAU_{avg} , both controllers presented similar values with slight variations and close to 69 and 4.2, respectively, which compared to those of a MPC with a perfect forecast ($IAE_{pf} = 60.969$ and $IAU_{pf} = 4.304$), they are close to IAU_{pf} but, because of uncertainties, considerably above IAE_{pf} . In some moments, in all the MPC simulations, the states exceeded their allowed limits. This was not the case for the applied inputs, which reached their allowed values without violating them.

4.2. Example 2

This example consists of a quadruple tank process [27] whose schematic diagram is depicted in Fig. 5 and whose control objective is to maintain the liquid level in the tank $T_i \forall i \in \{1, 2, 3, 4\}$ at a desired setpoint h_i by means of the flow rates Q_1 and Q_2 delivered by pumps 1 and 2, respectively. These flows are proportional to the applied voltage $Q_1 = k_1 v_1$, $Q_2 = k_2 v_2$ and are subsequently split by the valves in proportions determined by the parameters $\gamma_1, \gamma_2 \in [0, 1]$.

The nonlinear equations of this system and its discrete time linear model, for a sampling time $T_s = 5$ s, in the form Eq. (1a) are described in the Appendix and whose state $x = [x_1, x_2, x_3, x_4]^T$ and input $u = [u_1, u_2]^T$ vectors represent the deviations of the liquid levels in centimetres and voltages from the selected operating point, respectively.

The constraints on the system states are $[-1.2, -1.2]^T \leq [x_3, x_4]^T \leq [1.2, 1.2]^T$ cm, corresponding to the deviations in the liquid levels in tanks 3 and 4. Similarly, the constraints on the inputs are $[-1.0, -1.0]^T \leq [u_1, u_2]^T \leq [1.0, 1.0]^T$ V, which corresponds to the vari-

Table 3
Performance indices of the MPCs in Example 2 for a \mathbb{S}_S of 10,000 scenarios.

Controller	p_s	p_c	N_v	PD _{avg}	IAE _{avg}	IAU _{avg}	t_{avg}
ScMPC ₃₃₀	92.0%	96.6%	88	1.40%	76.702	18.772	678 ms
CSB-MPC ₃₃₀	92.7%	96.9%	79	1.32%	76.699	18.760	780 ms
ScMPC ₂₄₀	90.9%	96.2%	99	1.45%	76.703	18.777	463 ms
CSB-MPC ₂₄₀	92.5%	96.9%	82	1.37%	76.699	18.761	554 ms
ScMPC ₁₅₀	89.5%	95.6%	115	1.55%	76.707	18.789	314 ms
CSB-MPC ₁₅₀	91.2%	96.7%	95	1.40%	76.700	18.764	393 ms
ScMPC ₉₀	86.7%	94.8%	144	1.78%	76.712	18.804	205 ms
CSB-MPC ₉₀	89.0%	95.9%	118	1.51%	76.704	18.771	267 ms
ScMPC ₆₀	83.9%	94.0%	175	1.94%	76.718	18.823	154 ms
CSB-MPC ₆₀	85.9%	94.8%	152	1.68%	76.708	18.779	203 ms
ScMPC ₄₂	80.1%	92.8%	220	2.03%	76.728	18.848	78 ms
CSB-MPC ₄₂	80.8%	93.0%	213	1.84%	76.713	18.789	124 ms

ations in the voltages applied to the pumps 1 and 2. All uncertainties ($n_\delta = 6$) are stacked in the random vector $\delta = [\xi_1, \xi_2, \dots, \xi_6]^\top$, which has a truncated multivariate normal distribution $\delta \sim \mathcal{N}_6(\mu, \Sigma)$, with bounds $|\delta| \leq [0.01, 0.01, 0.17, 0.17, 0.17, 0.17]^\top$, mean vector $\mu = [0, 0, 0, 0, 0, 0]^\top$, and covariance matrix Σ with value

$$\Sigma = 10^{-3} \times \begin{bmatrix} 0.0250 & 0.0225 & 0 & 0 & 0 & 0 \\ 0.0225 & 0.0250 & 0 & 0 & 0 & 0 \\ 0 & 0 & 6.40 & 0 & 0 & 5.12 \\ 0 & 0 & 0 & 6.40 & 5.12 & 0 \\ 0 & 0 & 0 & 5.12 & 6.40 & 0 \\ 0 & 0 & 5.12 & 0 & 0 & 6.40 \end{bmatrix}.$$

4.2.1. Simulation setup

In this example, the performances of a ScMPC and a CSB-MPC for a primary set \mathbb{S}_S consisting of 10,000 and a smaller set of 1300 scenarios are compared. The numbers of scenarios selected are $M, C = \{330, 240, 150, 90, 60, 42\}$, which fulfil the condition $C = n_\delta E$ (see Assumption 3), and through Eq. (6), with $\beta = 10^{-9}$, their theoretical probabilities of constraints satisfaction $\mathbb{P}[x_{i+1} \in \mathbb{X}] \geq p_t$ are $p_t(M, C) = \{81.3\%, 74.9\%, 62.0\%, 42.5\%, 24.2\%, 9.0\%\}$. The duration of each simulation is 40 sampling periods for both MPCs and the nonlinear system initial state is $x_{0k}^{[j]} = \hat{x}_0 = [-6.7, -6.5, -1, -1]^\top$. The MPCs parameters are prediction horizon $N = 12$, cost function weights matrices $Q = \text{diag}(3, 3, 1, 1)$ and $R = I_2$. The robust invariant set \mathbb{X}_T consisting of a polytope of 54 hyperplanes, and K and P matrices are

$$K = \begin{bmatrix} -0.4824 & -0.4075 & -0.2635 & 0.0484 \\ -0.2867 & -0.3645 & 0.0402 & -0.3402 \end{bmatrix}, \quad P = \begin{bmatrix} 5.0037 & 2.0305 & -0.5713 & -0.4862 \\ 2.0305 & 5.0796 & -0.6271 & -0.4581 \\ -0.5713 & -0.6271 & 1.7320 & 0.1207 \\ -0.4862 & -0.4581 & 0.1207 & 1.5524 \end{bmatrix}.$$

4.2.2. Results

Tables 3 and 4 show the performance results of each MPC for cases $\mathbb{S}_S(10,000)$ and $\mathbb{S}_S(1300)$, respectively; where, as in Example 1, the first column corresponds to the type

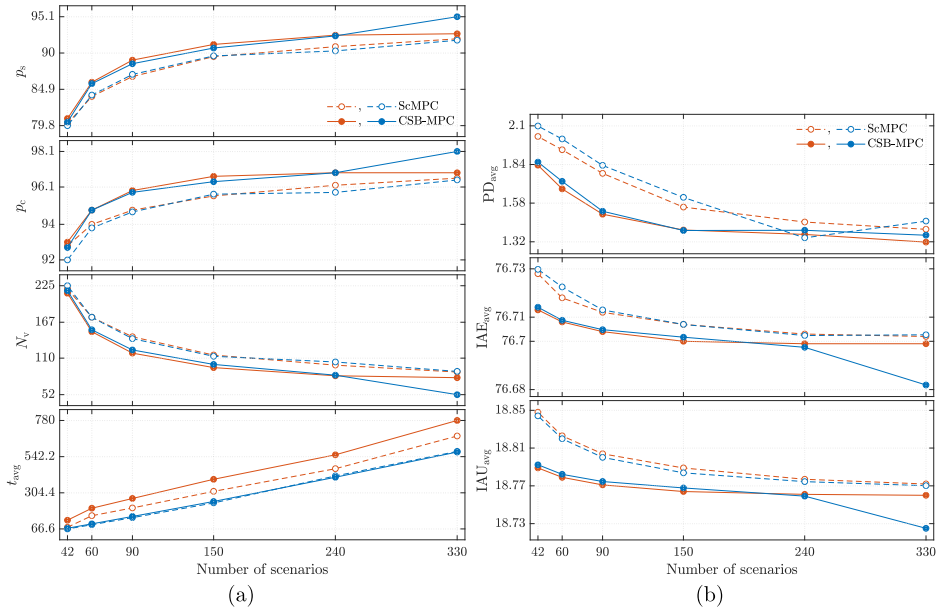


Fig. 6. Graphs of the performance indices from Tables 3 ($S_S(10,000)$, orange lines) and 4 ($S_S(1300)$, blue lines), corresponding to ScMPC (dashed lines) and CSB-MPC (solid lines), for 42, 60, 90, 150, 240 and 330 scenarios. (For interpretation of the references to colour in this figure legend, the reader is referred to the web version of this article.)

Table 4
Performance indices of the MPCs in Example 2 for a S_S of 1300 scenarios.

Controller	p_s	p_c	N_v	PD_{avg}	IAE_{avg}	IAU_{avg}	t_{avg}
ScMPC ₃₃₀	91.8%	96.5%	89	1.46%	76.703	18.770	577 ms
CSB-MPC ₃₃₀	95.1%	98.1%	52	1.36%	76.682	18.725	572 ms
ScMPC ₂₄₀	90.3%	95.8%	104	1.35%	76.702	18.775	415 ms
CSB-MPC ₂₄₀	92.4%	96.9%	83	1.40%	76.698	18.759	407 ms
ScMPC ₁₅₀	89.6%	95.7%	113	1.62%	76.707	18.784	238 ms
CSB-MPC ₁₅₀	90.7%	96.4%	100	1.40%	76.702	18.768	247 ms
ScMPC ₉₀	87.0%	94.7%	141	1.83%	76.713	18.800	141 ms
CSB-MPC ₉₀	88.5%	95.8%	123	1.53%	76.705	18.775	149 ms
ScMPC ₆₀	84.1%	93.8%	175	2.01%	76.723	18.820	95 ms
CSB-MPC ₆₀	85.7%	94.8%	155	1.73%	76.709	18.782	100 ms
ScMPC ₄₂	79.8%	92.0%	225	2.10%	76.730	18.844	67 ms
CSB-MPC ₄₂	80.3%	92.7%	217	1.86%	76.714	18.792	71 ms

of controller and the subsequent columns indicate the performance indices as defined at the beginning of this section (which were computed based on the N_r closed-loop responses of the nonlinear system). Furthermore, these indices are depicted in Fig. 6(a) and (b), in which the orange and blue lines represent those in Tables 3 and 4, respectively.

As in Example 1, it is verified that the CSB-MPCs obtained higher empirical probabilities of constraint satisfaction p_s and p_c than ScMPCs; and their p_s are significantly above the theoretical probabilities of constraint satisfaction p_t , signifying higher feasibility of an OCP solution, in a probabilistic sense. Moreover, the CSB-MPCs reported better N_v and PD_{avg}

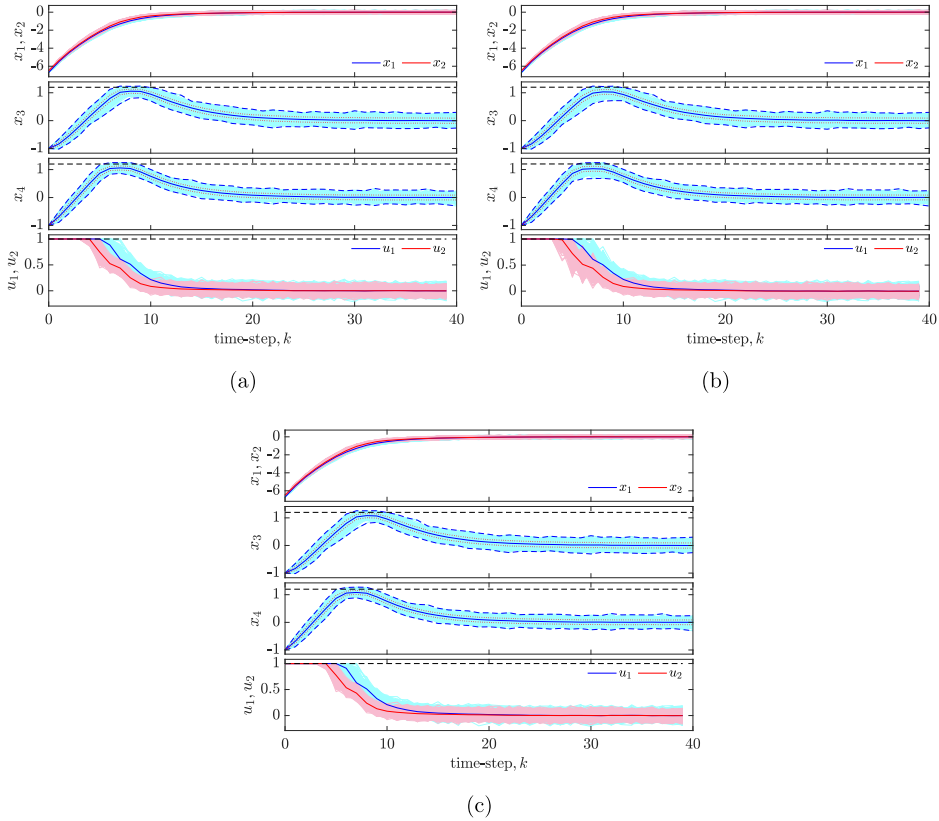


Fig. 7. Nonlinear system responses to a ScMPC₃₃₀, CSB-MPC₃₃₀ and CSB-MPC₄₂ controllers, for a \mathbb{S}_S of 1300 Scenarios. The 1000 closed-loop trajectories and applied inputs (thin solid lines), mean trajectory (thick solid lines), mean trajectory with standard deviation (dotted lines), minimum and maximum values (blue dashed lines) and constraints (black dashed lines) $|x_3|, |x_4| \leq 1.2, |u_1|, |u_2| \leq 1.0$. (a) ScMPC₃₃₀. (b) CSB-MPC₃₃₀. (c) CSB-MPC₄₂. (For interpretation of the references to colour in this figure legend, the reader is referred to the web version of this article.)

indices than the ScMPCs, except for the case $M, C = 240$ in Table 4, where the CSB-MPC obtained a slightly higher PD_{avg} , but with fewer constraints violated.

The closed-loop trajectories of the nonlinear system and the applied inputs for ScMPC₃₃₀, CSB-MPC₃₃₀, and CSB-MPC₄₂ in Table 4 are shown in Fig. 7(a)–(c), respectively. In Fig. 7(a) and (b), very similar behaviours are observed by both controllers; however, the best performances are presented by the CSB-MPC₃₃₀ (see Fig. 6). Comparing the performances of CSB-MPC₃₃₀ con CSB-MPC₄₂, it is noted that a decrease in the number of scenarios use to solve the OCP leads to an increase in the number of trajectories that violate the limits. Nevertheless, the mean trajectories with standard deviations (dotted lines) are kept within the limits (black dashed lines), indicating that the probability that a state is within the allowed limits is at least 68%.

As in Example 1, it is observed for a CSB-MPC that the solution time t_{avg} decreases significantly as the primary set becomes small, but does not significantly alter the probabilities p_s and p_c . This can be seen for the $\mathbb{S}_S(1300)$ case in Fig. 6(a), where the t_{avg} times of the

CSB-MPC are very close to those of a ScMPC, in some cases lower; e.g., CSB-MPC₂₄₀ and CSB-MPC₃₃₀ in Table 4. These CSB-MPCs mentioned, in addition to having shorter solution times t_{avg} than their corresponding ScMPC, have better p_s , p_c and N_v . In this way, with suitable size of \mathbb{S}_S , if an improvement of the time t_{avg} is required, a CSB-MPC is a viable alternative compared to a ScMPC. For example, if similar or superior performance indices to those of the ScMPC₃₃₀ ($t_{\text{avg}} = 577$ ms) in Table 4 are required, but with a lower solution time, the CSB-MPC₂₄₀ ($t_{\text{avg}} = 407$ ms) with a 170 ms quicker solution time could be used.

The lowest IAE_{avg} and IAU_{avg} indicators were obtained by the CSB-MPCs, although very similar to those of ScMPC at values close to $\text{IAE}_{\text{avg}} = 76.7$ and $\text{IAU}_{\text{avg}} = 18.8$, which compared to those of a MPC with a perfect forecast, they are close to $\text{IAE}_{\text{pf}} = 74.908$ and $\text{IAU}_{\text{pf}} = 19.440$. In the same way as in Example 1, the closed-loop trajectories exceeded their allowed limits at some moments in all the simulations in both controllers. The inputs applied initially reached their allowed maximums without transgressing them.

4.3. Final comments

As a summary of Examples 1 and 2, the results show that a CSB-MPC compared to a ScMPC with the same number of scenarios offers a better probability of constraint satisfaction and above the theoretical one, increasing the feasibility of an OCP solution, in a probabilistic sense. Such better probabilities of the CSB-MPC represent a decrease in the number of times constraints are violated and the deviation from the limits violated.

Furthermore, a decrease in the size of the primary set \mathbb{S}_S does not significantly alter the probabilities of constraints satisfaction in a CSB-MPC, but it can significantly reduce the time it takes for the OCP to find a solution, even close to that of a ScMPC, or in some cases smaller.

5. Conclusion

A novel model predictive control approach is introduced in this paper. This MPC scheme, called conditional scenario-based model predictive control (CSB-MPC), is designed for discrete-time linear systems affected by correlated and bound parametric uncertainties and/or additive disturbances. In this approach, a primary set of equiprobable and randomly generated scenarios is approximated to a set of conditional scenarios with their respective probabilities of occurrence. These are incorporated in the cost function of an optimal control problem where the predicted states and inputs are penalised according to the probabilities associated with the uncertainties on which they depend.

The performances of the CSB-MPC and those of a scenario-based MPC were compared using two numerical examples, whose results showed greater empirical probabilities of constraints satisfaction and less distance outside the constraints by the former, even when the CSB-MPCs have a smaller number of scenarios than the scenario-based MPCs. Moreover, for a smaller primary set, the CSB-MPC offers similar solution times, in some cases shorter than those of a standard scenario-based MPC. Consequently, if a trade-off between the level of constraints satisfaction and the computational tractability is required, using a CSB-MPC with a smaller number of scenarios than a scenario-based MPC is a viable option.

Future research directions will concentrate on issues such as defining the theoretical properties of feasibility and stability of the proposed approach, both for bounded and unbounded uncertainties; as well as analysing in more detail the influence of the prediction horizon

length, cost function weights, size of the primary set and the number of scenarios on the effectiveness of the technique in order to develop a selection principle for these parameters.

Declaration of Competing Interest

The authors declare that they have no known competing financial interests or personal relationships that could have appeared to influence the work reported in this paper.

Acknowledgements

This work was supported in part by the MCIN/ AEI/10.13039/501100011033 under Grant PID2020-120087GB-C21, and in part by the Ministry of Science, Technology and Innovation of Colombia under scholarship programme 885.

Appendix A

By performing a mass balance and applying Bernoulli’s law, the equations of the quadruple tank process [27] in Fig. 5 are

$$\begin{aligned}
 A_1 \dot{h}_1 &= -a_1 \sqrt{2gh_1} - a_{12} \operatorname{sgn}(\Delta h) \sqrt{2g|\Delta h|} + \beta_2 v_2 \\
 A_2 \dot{h}_2 &= -a_2 \sqrt{2gh_2} + a_{12} \operatorname{sgn}(\Delta h) \sqrt{2g|\Delta h|} + \beta_1 v_1 \\
 A_3 \dot{h}_3 &= a_1 \sqrt{2gh_1} - a_3 \sqrt{2gh_3} + \gamma_1 k_1 v_1 \\
 A_4 \dot{h}_4 &= a_2 \sqrt{2gh_2} - a_4 \sqrt{2gh_4} + \gamma_2 k_2 v_2
 \end{aligned}$$

where A_i and a_i are the cross section of the tank i and its base outlet pipe, respectively; a_{12} is the cross section of the pipe connecting T_1 and T_2 , g is the gravity; $\beta_1 = (1 - \gamma_1)k_1$, $\beta_2 = (1 - \gamma_2)k_2$ and $\Delta h = h_1 - h_2$.

By linearising the above equations around the operating point $P^o = \{h_1^o = 7.873 \text{ cm}, h_2^o = 8.187 \text{ cm}, h_3^o = 7.720 \text{ cm}, h_4^o = 8.039 \text{ cm}, v_1^o = 4.0 \text{ V}, v_2^o = 3.5 \text{ V}\}$ with $A_i = 144 \text{ cm}^2$; $a_1, a_2, a_{12} = 0.352 \text{ cm}^2$; $a_3 = 1.006 + \xi_1 \text{ cm}^2$, $a_4 = 1.006 + \xi_2 \text{ cm}^2$; $k_1, k_2 = 33.333 \text{ cm}^3/(\text{V}\cdot\text{s})$; $\gamma_1 = 0.6$, $\gamma_2 = 0.7$, $g = 981 \text{ cm/s}^2$. By discretising with a sampling time $T_s = 5 \text{ s}$ the resulting equations using Euler’s approximation, and taking into account additive disturbances caused by other hydraulic connections, we obtain the discrete time model of the form Eq. (1a)

$$x_{i+1} = A(\delta_i)x_i + Bu_i + Gw(\delta_i)$$

with

$$\begin{aligned}
 A(\delta_i) &= \begin{bmatrix} 0.421 & 0.483 & 0 & 0 \\ 0.483 & 0.422 & 0 & 0 \\ 0.097 & 0 & 0.722 - 0.277\xi_{1,i} & 0 \\ 0 & 0.095 & 0 & 0.727 - 0.271\xi_{2,i} \end{bmatrix}, \\
 B &= \begin{bmatrix} 0 & 0.347 \\ 0.463 & 0 \\ 0.694 & 0 \\ 0 & 0.810 \end{bmatrix}, \quad G = I_4.
 \end{aligned}$$

Here the state $x = [x_1, x_2, x_3, x_4]^T$ and input $u = [u_1, u_2]^T$ vectors represent the deviations of the liquid levels and voltages from P^o , respectively (e.g., $x_1 = h_1 - h_1^o$, $u_1 = v_1 - v_1^o$) and the variables ξ represent the uncertainties and $w(\delta_i) = [\xi_{3,i}, \xi_{4,i}, \xi_{5,i}, \xi_{6,i}]^T$.

References

- [1] M.G. Forbes, R.S. Patwardhan, H. Hamadah, R.B. Gopaluni, Model predictive control in industry: challenges and opportunities, *IFAC-PapersOnLine* 48 (8) (2015) 531–538, doi:[10.1016/j.ifacol.2015.09.022](https://doi.org/10.1016/j.ifacol.2015.09.022).
- [2] J. Rodríguez, M.P. Kazmierkowski, J.R. Espinoza, P. Zanchetta, H. Abu-Rub, H.A. Young, C.A. Rojas, State of the art of finite control set model predictive control in power electronics, *IEEE Trans. Ind. Inf.* 9 (2) (2013) 1003–1016, doi:[10.1109/tii.2012.2221469](https://doi.org/10.1109/tii.2012.2221469).
- [3] A. Parisio, D. Varagnolo, M. Molinari, G. Pattarello, L. Fabbietti, K.H. Johansson, Implementation of a scenario-based MPC for HVAC systems: an experimental case study, *IFAC Proc.* Vol. 47 (3) (2014) 599–605, doi:[10.3182/20140824-6-za-1003.02629](https://doi.org/10.3182/20140824-6-za-1003.02629).
- [4] I. Ravanshadi, E.A. Boroujeni, M. Pourgholi, Centralized and distributed model predictive control for consensus of non-linear multi-agent systems with time-varying obstacle avoidance, *ISA Trans.* (2022) 1–13, doi:[10.1109/tcst.2017.2657606](https://doi.org/10.1109/tcst.2017.2657606).
- [5] H.G. Tanner, J.L. Piovesan, Randomized receding horizon navigation, *IEEE Trans. Autom. Control* 55 (11) (2010) 2640–2644, doi:[10.1109/tac.2010.2063291](https://doi.org/10.1109/tac.2010.2063291).
- [6] P. Velarde, A.J. Gallego, C. Bordons, E.F. Camacho, Scenario-based model predictive control for energy scheduling in a parabolic trough concentrating solar plant with thermal storage, *Renew. Energy* 206 (2023) 1228–1238, doi:[10.1016/j.renene.2023.02.114](https://doi.org/10.1016/j.renene.2023.02.114).
- [7] M.V. Kothare, V. Balakrishnan, M. Morari, Robust constrained model predictive control using linear matrix inequalities, *Automatica* 32 (10) (1996) 1361–1379, doi:[10.1016/0005-1098\(96\)00063-5](https://doi.org/10.1016/0005-1098(96)00063-5).
- [8] B. Kouvaritakis, M. Cannon, Developments in robust and stochastic predictive control in the presence of uncertainty, *ASCE-ASME J. Risk Uncertain. Eng. Syst.* 1 (2) (2015) 1–9, doi:[10.1115/1.4029744](https://doi.org/10.1115/1.4029744).
- [9] A. Mesbah, Stochastic model predictive control: an overview and perspectives for future research, *IEEE Control Syst. Mag.* 36 (6) (2016) 30–44, doi:[10.1109/MCS.2016.2602087](https://doi.org/10.1109/MCS.2016.2602087).
- [10] B. Kouvaritakis, M. Cannon, *Model Predictive Control. Classical, Robust and Stochastic*, first ed., Springer International Publishing, 2016, doi:[10.1007/978-3-319-24853-0](https://doi.org/10.1007/978-3-319-24853-0).
- [11] M. Farina, L. Giulioni, R. Scattolini, Stochastic linear model predictive control with chance constraints—A review, *J. Process Control* 44 (2016) 53–67, doi:[10.1016/j.procont.2016.03.005](https://doi.org/10.1016/j.procont.2016.03.005).
- [12] M. Lorenzen, F. Dabbene, R. Tempo, F. Allgöwer, Stochastic MPC with offline uncertainty sampling, *Automatica* 81 (2017) 176–183, doi:[10.1016/j.automatica.2017.03.031](https://doi.org/10.1016/j.automatica.2017.03.031).
- [13] H. Wang, J. Wang, H. Xu, S. Zhao, Distributed stochastic model predictive control for systems with stochastic multiplicative uncertainty and chance constraints, *ISA Trans.* 121 (2022) 11–20, doi:[10.1016/j.isatra.2021.03.038](https://doi.org/10.1016/j.isatra.2021.03.038).
- [14] B. Kouvaritakis, M. Cannon, *Stochastic Model Predictive Control*, first ed., Springer London, London, U.K., 2015, pp. 1350–1357.
- [15] L.M. Chaouach, M. Fiacchini, T. Alamo, Stochastic model predictive control for linear systems affected by correlated disturbances, *IFAC-PapersOnLine* 55 (25) (2022) 133–138, doi:[10.1016/j.ifacol.2022.09.336](https://doi.org/10.1016/j.ifacol.2022.09.336).
- [16] M. Mammarella, T. Alamo, S. Lucia, F. Dabbene, A probabilistic validation approach for penalty function design in stochastic model predictive control, *IFAC-PapersOnLine* 53 (2) (2020) 11271–11276, doi:[10.1016/j.ifacol.2020.12.362](https://doi.org/10.1016/j.ifacol.2020.12.362).
- [17] F. Li, H. Li, Y. He, Stochastic model predictive control for linear systems with unbounded additive uncertainties, *J. Frankl. Inst.* 359 (7) (2022) 3024–3045, doi:[10.1016/j.franklin.2022.02.004](https://doi.org/10.1016/j.franklin.2022.02.004).
- [18] G.C. Calafiore, L. Fagiano, Robust model predictive control via scenario optimization, *IEEE Trans. Autom. Control* 58 (1) (2013) 219–224, doi:[10.1109/tac.2012.2203054](https://doi.org/10.1109/tac.2012.2203054).
- [19] G. Schildbach, L. Fagiano, C. Frei, M. Morari, The scenario approach for stochastic model predictive control with bounds on closed-loop constraint violations, *Automatica* 50 (12) (2014) 3009–3018, doi:[10.1016/j.automatica.2014.10.035](https://doi.org/10.1016/j.automatica.2014.10.035).
- [20] F. Micheli, J. Lygeros, Scenario-based stochastic MPC for systems with uncertain dynamics, in: *2022 European Control Conference (ECC)*, IEEE, 2022, doi:[10.23919/ecc55457.2022.9838080](https://doi.org/10.23919/ecc55457.2022.9838080).
- [21] M. Kögel, R. Findeisen, Robust output feedback MPC for uncertain linear systems with reduced conservatism, *IFAC-PapersOnLine* 50 (1) (2017) 10685–10690, doi:[10.1016/j.ifacol.2017.08.2186](https://doi.org/10.1016/j.ifacol.2017.08.2186).

- [22] M. Lorenzen, F. Dabbene, R. Tempo, F. Allgöwer, Constraint-tightening and stability in stochastic model predictive control, *IEEE Trans. Autom. Control* 62 (7) (2017) 3165–3177, doi:[10.1109/TAC.2016.2625048](https://doi.org/10.1109/TAC.2016.2625048).
- [23] M. Cannon, B. Kouvaritakis, S.V. Raković, Q. Cheng, Stochastic tubes in model predictive control with probabilistic constraints, *IEEE Trans. Autom. Control* 56 (1) (2011) 194–200, doi:[10.1109/TAC.2010.2086553](https://doi.org/10.1109/TAC.2010.2086553).
- [24] T.A.N. Heirung, J.A. Paulson, J. O’Leary, A. Mesbah, Stochastic model predictive control - how does it work? *Comput. Chem. Eng.* 114 (2018) 158–170, doi:[10.1016/j.compchemeng.2017.10.026](https://doi.org/10.1016/j.compchemeng.2017.10.026).
- [25] A. Mesbah, Stochastic model predictive control with active uncertainty learning: a survey on dual control, *Annu. Rev. Control* 45 (2018) 107–117, doi:[10.1016/j.arcontrol.2017.11.001](https://doi.org/10.1016/j.arcontrol.2017.11.001).
- [26] L. Hewing, M.N. Zeilinger, Scenario-based probabilistic reachable sets for recursively feasible stochastic model predictive control, *IEEE Control Syst. Lett.* 4 (2) (2020) 450–455, doi:[10.1109/lcsys.2019.2949194](https://doi.org/10.1109/lcsys.2019.2949194).
- [27] E. González, J. Sanchis, S. García-Nieto, J. Salcedo, A comparative study of stochastic model predictive controllers, *Electronics* 9 (12) (2020) 2078, doi:[10.3390/electronics9122078](https://doi.org/10.3390/electronics9122078).
- [28] J.M. Grosso, P. Velarde, C. Ocampo-Martinez, J.M. Maestre, V. Puig, Stochastic model predictive control approaches applied to drinking water networks, *Optim. Control Appl. Methods* 38 (4) (2016) 541–558, doi:[10.1002/oca.2269](https://doi.org/10.1002/oca.2269).
- [29] M.M. Seron, G.C. Goodwin, D.S. Carrasco, Stochastic model predictive control: insights and performance comparisons for linear systems, *Int. J. Robust Nonlinear Control* 29 (2019) 5038–5057, doi:[10.1002/rnc.4106](https://doi.org/10.1002/rnc.4106).
- [30] G. Calafiore, M.C. Campi, The scenario approach to robust control design, *IEEE Trans. Autom. Control* 51 (5) (2006) 742–753, doi:[10.1109/tac.2006.875041](https://doi.org/10.1109/tac.2006.875041).
- [31] M.C. Campi, S. Garatti, M. Prandini, The scenario approach for systems and control design, *Annu. Rev. Control* 33 (2) (2009) 149–157, doi:[10.1016/j.arcontrol.2009.07.001](https://doi.org/10.1016/j.arcontrol.2009.07.001).
- [32] A. Muralledharan, H. Okuda, T. Suzuki, Real-time implementation of randomized model predictive control for autonomous driving, *IEEE Trans. Intell. Veh.* 7 (1) (2022) 11–20, doi:[10.1109/tiv.2021.3062730](https://doi.org/10.1109/tiv.2021.3062730).
- [33] H.A. Nasir, M. Cantoni, Y. Li, E. Weyer, Stochastic model predictive control based reference planning for automated open-water channels, *IEEE Trans. Control Syst. Technol.* 29 (2) (2021) 607–619, doi:[10.1109/tcst.2019.2952788](https://doi.org/10.1109/tcst.2019.2952788).
- [34] S. Polimeni, L. Meraldi, L. Moretti, S. Leva, G. Manzolini, Development and experimental validation of hierarchical energy management system based on stochastic model predictive control for off-grid microgrids, *Adv. Appl. Energy* 2 (2021) 100028, doi:[10.1016/j.adapen.2021.100028](https://doi.org/10.1016/j.adapen.2021.100028).
- [35] M.C. Campi, S. Garatti, A sampling-and-discarding approach to chance-constrained optimization: feasibility and optimality, *J. Optim. Theory Appl.* 148 (2) (2010) 257–280, doi:[10.1007/s10957-010-9754-6](https://doi.org/10.1007/s10957-010-9754-6).
- [36] D. Bernardini, A. Bemporad, Scenario-based model predictive control of stochastic constrained linear systems, in: *Proceedings of the 48th IEEE Conference on Decision and Control (CDC) held jointly with 2009 28th Chinese Control Conference, Shanghai, China, 2009*, pp. 6333–6338, doi:[10.1109/cdc.2009.5399917](https://doi.org/10.1109/cdc.2009.5399917).
- [37] A. Mesbah, I.V. Kolmanovskiy, S.D. Cairano, *Stochastic Model Predictive Control*, first ed., Springer International Publishing, 2018, pp. 75–97.
- [38] A.D. Bonzanini, J.A. Paulson, A. Mesbah, Safe learning-based model predictive control under state- and input-dependent uncertainty using scenario trees, in: *2020 59th IEEE Conference on Decision and Control (CDC)*, IEEE, Jeju, Korea (South), 2020, doi:[10.1109/cdc42340.2020.9304310](https://doi.org/10.1109/cdc42340.2020.9304310).
- [39] Y. Bao, K.J. Chan, A. Mesbah, J.M. Velni, Learning-based adaptive-scenario-tree model predictive control with improved probabilistic safety using robust Bayesian neural networks, *Int. J. Robust Nonlinear Control* 33 (5) (2022) 3312–3333, doi:[10.1002/rnc.6560](https://doi.org/10.1002/rnc.6560).
- [40] P. Velarde, L. Valverde, J. Maestre, C. Bordons, On the comparison of stochastic model predictive control strategies applied to a hydrogen-based microgrid, *J. Power Sources* 343 (2017) 161–173, doi:[10.1016/j.jpowsour.2017.01.015](https://doi.org/10.1016/j.jpowsour.2017.01.015).
- [41] D. Mayne, Robust and stochastic MPC: are we going in the right direction? *IFAC-PapersOnLine* 48 (23) (2015) 1–8, doi:[10.1016/j.ifacol.2015.11.255](https://doi.org/10.1016/j.ifacol.2015.11.255).
- [42] D. Mayne, J. Rawlings, C. Rao, P. Scokaert, Constrained model predictive control: stability and optimality, *Automatica* 36 (6) (2000) 789–814, doi:[10.1016/S0005-1098\(99\)00214-9](https://doi.org/10.1016/S0005-1098(99)00214-9).
- [43] G.C. Calafiore, Random convex programs, *SIAM J. Optim.* 20 (6) (2010) 3427–3464, doi:[10.1137/090773490](https://doi.org/10.1137/090773490).
- [44] F. Blanchini, Set invariance in control, *Automatica* 35 (11) (1999) 1747–1767, doi:[10.1016/S0005-1098\(99\)00113-2](https://doi.org/10.1016/S0005-1098(99)00113-2).
- [45] D.Q. Mayne, P. Falugi, Stabilizing conditions for model predictive control, *Int. J. Robust Nonlinear Control* 29 (4) (2018) 894–903, doi:[10.1002/rnc.4409](https://doi.org/10.1002/rnc.4409).
- [46] J. Rawlings, *Model Predictive Control: Theory, Computation, and Design*, second ed., Nob Hill Publishing, Madison, Wisconsin, U.S., 2017.

- [47] S. Boyd, L. El Ghaoui, E. Feron, V. Balakrishnan, *Linear Matrix Inequalities in System and Control Theory*, Society for Industrial and Applied Mathematics, Philadelphia, U.S., 1994, doi:[10.1137/1.9781611970777](https://doi.org/10.1137/1.9781611970777).
- [48] J. Maciejowski, *Predictive Control: With Constraints*, first ed., Prentice Hall, London, U.K., 2002.
- [49] C. Beltran-Royo, Two-stage stochastic mixed-integer linear programming: the conditional scenario approach, *Omega* 70 (2017) 31–42, doi:[10.1016/j.omega.2016.08.010](https://doi.org/10.1016/j.omega.2016.08.010).
- [50] C. Beltran-Royo, Two-stage stochastic mixed-integer linear programming: from scenarios to conditional scenarios, *Optimization* (2018) 1–30. Online <https://optimization-online.org/>.
- [51] C. Beltran-Royo, Fast scenario reduction by conditional scenarios in two-stage stochastic MILP problems, *Optim. Methods Softw.* 0 (0) (2019) 1–22, doi:[10.1080/10556788.2019.1697696](https://doi.org/10.1080/10556788.2019.1697696).
- [52] C. Beltran-Royo, From scenarios to conditional scenarios in two-stage stochastic MILP problems, *Int. Trans. Oper. Res.* 28 (2) (2020) 660–686, doi:[10.1111/itor.12851](https://doi.org/10.1111/itor.12851).
- [53] A.J. Kleywegt, A. Shapiro, T. Homem-de-Mello, The sample average approximation method for stochastic discrete optimization, *SIAM J. Optim.* 12 (2) (2002) 479–502, doi:[10.1137/s1052623499363220](https://doi.org/10.1137/s1052623499363220).
- [54] J. Dupačová, N. Gröwe-Kuska, W. Römisch, Scenario reduction in stochastic programming, *Math. Program.* 95 (3) (2003) 493–511, doi:[10.1007/s10107-002-0331-0](https://doi.org/10.1007/s10107-002-0331-0).
- [55] M. ApS, The MOSEK optimization toolbox for MATLAB manual. Version 9.0., 2019. <http://docs.mosek.com/9.0/toolbox/index.html>.
- [56] J. Löfberg, Automatic robust convex programming, *Optim. Methods Softw.* 27 (1) (2012) 115–129, doi:[10.1080/10556788.2010.517532](https://doi.org/10.1080/10556788.2010.517532).
- [57] M. Kvasnica, B. Takács, J. Holaza, D. Ingole, Reachability analysis and control synthesis for uncertain linear systems in MPT, *IFAC-PapersOnLine* 48 (14) (2015) 302–307, doi:[10.1016/j.ifacol.2015.09.474](https://doi.org/10.1016/j.ifacol.2015.09.474).
- [58] E.A. González Querubín, CSB-MPC. Version 1.0.1, 2021, <https://www.mathworks.com/matlabcentral/fileexchange/102224>.